Distribution, Structure, and Dynamics of Cesium and Iodide Ions at the H_2O-CCl_4 and H_2O−Vapor Interfaces

Collin D. Wick and Liem X. Dang*

Chemical Sciences Division, Pacific Northwest National Laboratory, Richland, Washington 99352

Received: September 23, 2005; In Final Form: January 29, 2006

Molecular dynamics simulations utilizing many-body potentials of H_2O-CCl_4 and H_2O−vapor interfaces were carried out at different cesium and iodide ion concentrations to compare ion distribution, interfacial orientational and structural properties, and dynamics. It was found that cesium was repelled by both interfaces, and iodide was active at both interfaces, but to a much greater degree at the H_2O−vapor interface. At the interface, the iodide dipole was strongly induced, orienting perpendicular to the interface for both systems, leading to stronger hydrogen bonds with water. For the H_2O-CCl_4 interface, though, there was a compensation between these strong hydrogen bonds and short to moderate ranged repulsion between iodide and CCl_4. Hydrogen bond distance and angular distributions showed weaker water−water hydrogen bonds at both interfaces, but generally stronger water−iodide hydrogen bonds. Both translational and rotational dynamics of water were faster at the interface, while for CCl_4, its translational dynamics was slower, but rotational dynamics faster at the interface. For many of the studied systems and species, translational diffusion was found to be anisotropic at both interfacial and bulk regions.

I. Introduction

The interactions and distribution of ions at organic−aqueous and vapor−aqueous interfaces are of high importance for a variety of biological, chemical, and atmospheric processes.[1−3] For instance, molecular uptake and dynamics of ions in the interfacial region of aerosols will have an effect on atmospheric composition.[4] The interaction of contaminated solvents in groundwater and their separation will be affected by the distribution of ions at liquid−liquid interfaces.[5] Additionally, the efficiency of drug delivery will be influenced by aqueous−organic interfacial properties in the presence of ions. A detailed understanding of the microscopic structure of all species, including their distributions, at these interfaces is important for the optimization and development for these areas.

There has been a considerable amount of research targeted at the study of alkali−halide ion distributions at vapor−aqueous and organic−aqueous phases. These include molecular simulation studies utilizing polarizable potentials[6−10] and recent experimental studies[11−14] of the air−water interface. These studies have determined that while alkali cations are generally repelled by the interface, certain halide anions are surface active. This surface activity was determined to be the result of anions having increased dipoles due to their polarizabilities at the vapor−aqueous interface increasing their free energies in the region.[6−10] Studies of alkali−halide ions at the liquid−liquid interface are not as prevalent, though, with only a few of the molecular simulation studies utilizing nonpolarizable potentials.[15,16] Because these simulations did not extensively use polarizable potentials, the consequences of ion polarizabilities on interfacial effects, which have been found to be very important for vapor−aqueous systems, could not be investigated. The inclusion of ion and molecular polarizabilities will likely have a significant effect on the ion distributions at organic−aqueous interfaces, and lend significant new insight on the driving forces for ion distributions

Influenced by the importance for determining ion distributions at different interfaces, and their effect on local dynamics and structure, the current study aims to develop an understanding of alkali−halide ionic distributions at aqueous−vapor and aqueous−organic interfaces. The ions of choice are cesium and iodide, in which cesium was chosen because of its importance for nuclear waste remediation[17] and iodide was chosen because of its high surface activity in aqueous−vapor systems.

II. Computational Details

The species modeled were water, carbon tetrachloride, and cesium and iodide ions, with a combination of Lennard-Jones (LJ), electrostatic, and polarizable intermolecular potentials used to model molecular interactions. The water potential used was the four site rigid Dang−Chang water model,[18,19] which has O−H bond lengths of 0.9572 Å and a H−O−H angle of 104.5°. Positive electrostatic interaction sites are located at the hydrogen atomic positions, and a negatively charged *m* site with a point polarizability is located along the H−O−H bisector at a distance of 0.215 Å from the oxygen atomic position. In addition, a LJ site is located at the oxygen atomic position. For carbon tetrachloride, a rigid five site tetrahedral model was used,[20] with C−Cl bond lengths of 1.77 Å, positive charges on the chloride atomic positions, and a negative site on the carbon atomic position. LJ sites and point polarizabilities are located at all atomic positions. Both water and carbon tetrachloride had their geometries fixed with use of the SHAKE algorithm.[21] The cesium[22] and iodide[8] ions had positive and negative charges, respectively, LJ interaction sites, and point polarizabilities located at their atomic positions. The specific values used for the LJ, electrostatic, and point polarizabilities can be found in their respective references for water,[19] carbon tetrachloride,[20] and cesium[22] and iodide[8] ions. An iterative self-consistent field

* Address correspondence to this author.

10.1021/jp055427c CCC: $33.50
Published on Web 03/15/2006

procedure was used to evaluate the point polarizabilities, in which the induced dipoles arising from the polarizabilities are modified until deviations in sequential iterations are less than 0.00001 D.

Four separate molecular dynamics simulations were carried out at a temperature of 298 K with a heat bath coupling of 0.1 ps.[23] All simulations had two interfaces, distributed along the *z*-axis, with periodic liquid in the *x* and *y* directions. The four simulations included one with no carbon tetrachloride, forming only vapor−aqueous interfaces, and three with carbon tetrachloride, which formed organic−aqueous interfaces. The three simulations with carbon tetrachloride included 2669 water molecules and 500 carbon tetrachloride molecules, and the number of ions present in the simulations was varied. One simulation had no ions present, one had 48 of each kind, corresponding to a 1 M CsI aqueous solution, and the other had 144 of each ion, corresponding to a 3 M CsI aqueous solution. The system without carbon tetrachloride had 1000 water molecules and 18 of each ion, corresponding to a 1 M CsI aqueous solution. Since these are highly interfacial systems, the use of molarity is not totally correct, since ions are not evenly distributed between the interface and bulk, resulting in a bulk molarity not equal to the values given, but the notation of molarity is used here for convenience.

All simulations were equilibrated from initially pure (either water or water and carbon tetrachloride) equilibrated simulations from previous studies. The addition of cesium and iodide progressed by slowly adding ions, one pair per 0.01 ps, choosing the most energetically favorable position out of 1000 random trial positions, restricting the trialed positions to be within 4 Å of a water molecule. This procedure was done to create two separate and independent configurations for each simulation set. The simulations with carbon tetrachloride were then equilibrated for 500 ps at a constant pressure of 1 atm, with pressure relaxation of 0.2 ps.[23] The simulations without carbon tetrachloride were equilibrated for 500 ps at constant volume, with the aqueous liquid occupying a third of the simulation box. Following equilibration, 2.5 ns of production at constant volume were carried out for the three simulations with ions, and 1.5 ns of production for the simulation without. A potential truncation of 9 Å was used for the LJ interactions, and the particle mesh Ewald summation technique was used to handle long-ranged electrostatics.

III. Results and Discussion

A. Density Profiles. Density profiles for all systems simulated are given in Figure 1, showing a significant amount of iodide present at both the H_2O-CCl_4 and H_2O−vapor interfaces. The interfacial positions were determined by fitting to the following hyperbolic tangent functional form[24]

$$\rho(z) = \frac{1}{2}(\rho_I + \rho_{II}) - \frac{1}{2}(\rho_I - \rho_{II}) \tanh[(z - z_0)/d] \qquad (1)$$

where ρ_I and ρ_{II} are the bulk densities in phases I and II, respectively, z_0 is the position of the Gibb's dividing surface, and d estimates the interfacial thickness. The Gibbs dividing surface used in all figures is determined from water for all systems.

Comparing the systems with ions present, it can clearly be observed that the iodide density is much higher at the H_2O−vapor interface than the 1 M H_2O-CCl_4 interface, and is similar to the iodide density at the 3 M H_2O-CCl_4 interface, despite its overall iodide concentration being a third as high. This allows one to conclude that iodide is surface active at the H_2O-CCl_4 interface, but not nearly to the degree as at the H_2O−vapor interface. Additionally, the iodide density peak at the H_2O−vapor interface is sharper than that at the H_2O-CCl_4 interface, which has an iodide density peak that is broader toward the water bulk. There is not a significant amount of cesium present at any of the simulated interfaces, with its density peaking near the position where the water density begins to decrease from its bulk value. This small cesium density peak is likely due to the density peak of iodide in the interfacial region, and is stronger near the H_2O−vapor interface, where the iodide density peak is sharper.

The CCl_4 density distribution shows similar structures for all three H_2O-CCl_4 systems, but with increased ion concentration, CCl_4 appears to be "pushed" farther away from the water Gibb's dividing surface. The H_2O-CCl_4 and iodide$-CCl_4$ dimer energies as a function of heavy atom interatomic distance are given in Figure 2. The energies show that up to moderate ranges, the iodide$-CCl_4$ dimer energy is positive in value, and while the H_2O-CCl_4 energy is never very favorable, it is lower in energy than iodide$-CCl_4$ up to around 4 Å. This lends insight into why the presence of iodide at the interface "pushes" CCl_4 away from the water Gibb's dividing surface. Apparently, for the H_2O-CCl_4 systems, there is compensation between the favorableness of iodide to be in the interfacial water region and the short-ranged (but longer ranged than H_2O-CCl_4) repulsive interactions between iodide and CCl_4. This results in a decrease in the amount of iodide at the H_2O-CCl_4 interfacial region, compared with that at the H_2O−vapor interface. This also is likely responsible for the effect of "pushing" CCl_4 away from the water Gibb's dividing surface.

B. Radial Distribution Functions. Oxygen−oxygen and carbon−carbon radial distribution functions (RDFs) for the 1 M CsI H_2O-CCl_4 and H_2O−vapor systems are given in Figure 3. The RDFs were calculated in slabs of 2.5 Å along the *z*-axis. Target atoms are assigned regions in which they reside, and the average atomic density within 12 Å of the assigned region normalizes the distribution of atoms surrounding the target atom. This results in the RDFs approaching one for all regions. The interfacial region for the oxygen−oxygen RDFs was defined between −5 and 2.5 Å of the interface, and between −2.5 and 5 Å for the carbon−carbon RDFs, with negative values corresponding with the water phase. The most noticeable difference between the interfacial and bulk RDFs are their higher first peaks at the interfaces. This is due to the fact that while the overall density decreases at the interface, the number of nearest neighbors of the same type for either oxygen or carbon decreases at a lesser rate. The first peaks for the oxygen−oxygen RDFs for the H_2O−vapor system are slightly lower than the same RDFs for the H_2O-CCl_4 at both the bulk and interface, which may be due to lingering effects from the interfaces. The pure and 3 M CsI H_2O-CCl_4 systems gave RDFs (not shown for clarity) that were nearly identical with the RDFs for the 1 M CsI H_2O-CCl_4 system.

Figure 4 gives the ion pair RDFs in the bulk and interfacial regions, corresponding with the probability to find iodide ions surrounding a cesium. Increased ion concentration results in a lower first RDF peak, which is similar to the origin for the increase in the first oxygen−oxygen RDF peak at the interface, in which the overall density increases faster than the number of nearest neighbors. Furthermore, the first RDF peak is much higher at the interface, corresponding to the region where the iodide concentration is the highest. This runs counter to the previous observations of the oxygen−oxygen and carbon−carbon RDFs (which have lower oxygen and carbon densities

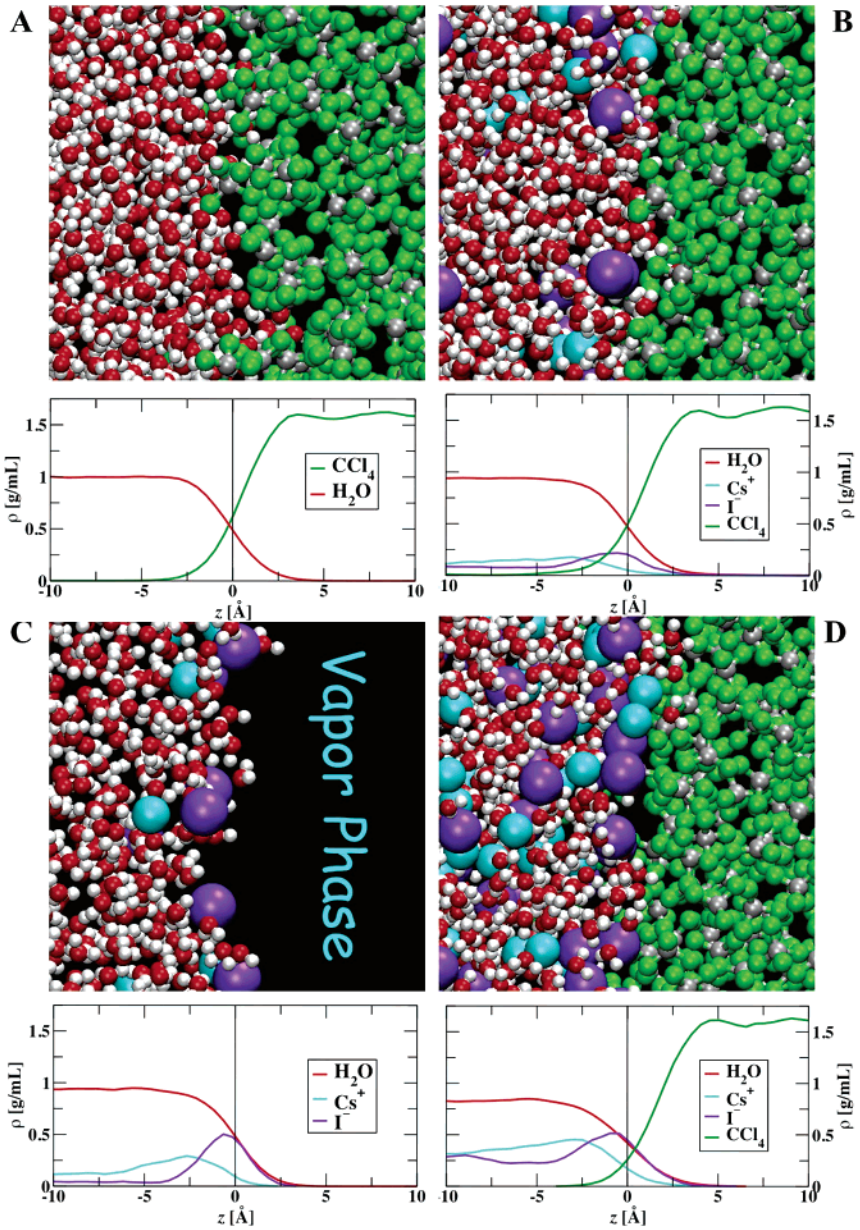

Figure 1. Snapshots and specific densities as a function of position with respect to the Gibb's dividing surface of water (at zero), with negative values representing the water phase, and positive values representing either carbon tetrachloride or vapor. The pure, 1 M CsI, and 3 M CsI H_2O-CCl_4 systems are represented in A, B, and D, respectively, while the 1 M CsI H_2O−vapor system is represented in C.

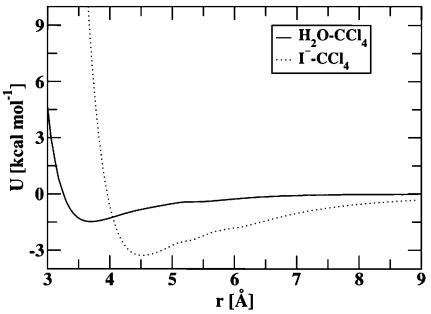

Figure 2. Dimer energies as a function of distance for H_2O-CCl_4 and iodide$-CCl_4$ pairs.

at the interface), suggesting a noticeably higher degree of ion association in the interfacial region. In addition, while the first RDF peaks are similar for the 1 M vapor$-H_2O$ and H_2O-CCl_4 systems in the bulk, the first CsI RDF peak for the H_2O-CCl_4 system is much higher than that for the vapor$-H_2O$ system.

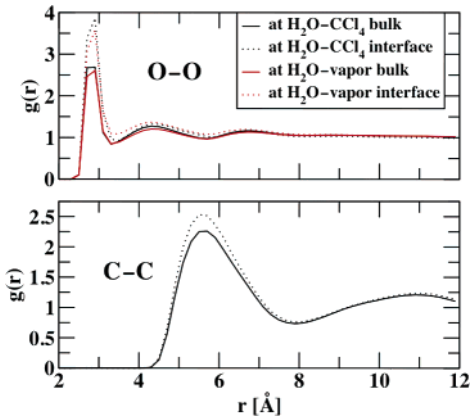

Figure 3. Oxygen−oxygen RDFs (top) and carbon−carbon RDFs (bottom) for 1 M CsI systems.

The number of iodide ions within the first solvation shell of cesium (4.5 Å) was determined for the interfacial and bulk

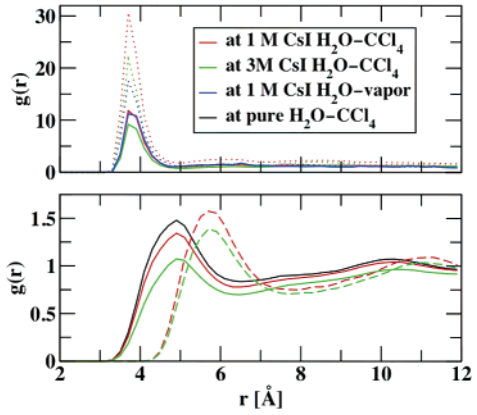

Figure 4. Cesium−iodide RDFs (top) for bulk (solid lines) and interface (dotted lines) and interfacial oxygen−carbon (bottom, solid lines) and iodide-carbon (bottom, dashed lines) RDFs.

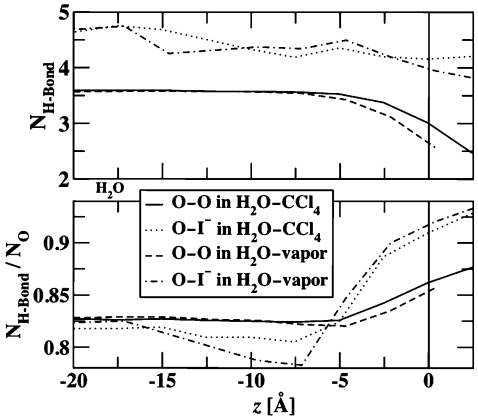

Figure 5. Number of hydrogen bonds (top) and the number of hydrogen bonds divided by the number of oxygens in the first solvation shell (bottom) as a function of position for water and iodide for the 1 M CsI systems.

regions, giving an interfacial-to-bulk ratio of 1.9 for the 1 M CsI H_2O-CCl_4 and 1.7 for the 1 M CsI H_2O−vapor system, being fairly close. The specific density interfacial-to-bulk ratio for the two systems was 1.4 and 3.7, respectively, bringing insight into why there is a much higher first peak in the interfacial RDF, which is related to the number of nearest neighbors divided by average density, for the 1 M CsI H_2O-CCl_4 system. From these results, it is evident that the strength of CsI ion pairing is greater at the H_2O-CCl_4 interface than at the H_2O-vapor interface, and ion pairing is lowest in bulk water.

Figure 4 gives the RDFs for the distribution of CCl_4 carbons around H_2O oxygens and iodide for the interfacial region of the H_2O-CCl_4 systems, showing that the first oxygen−carbon RDF peaks are at shorter distances, which is expected from the dimer energy calculations. Another interesting feature is that the first RDF peaks for both oxygen−carbon and iodide−carbon decrease with increased ion concentration. This is consistent with the observations of the density profiles, which show that CCl_4 is "pushed" away from the water Gibb's dividing surface with higher ion concentration, leading to the likelihood that increased ion concentration slightly impedes the interactions of water with CCl_4.

Figure 5 gives the number of hydrogen bonds as a function of position for water and iodide for the 1 M CsI H_2O-CCl_4 and H_2O−vapor systems, along with the ratio of hydrogen bonds to the number of oxygens within the first solvation shell. A hydrogen bond between two waters was defined when their oxygen−oxygen distance was less than 3.4 Å (defined as first

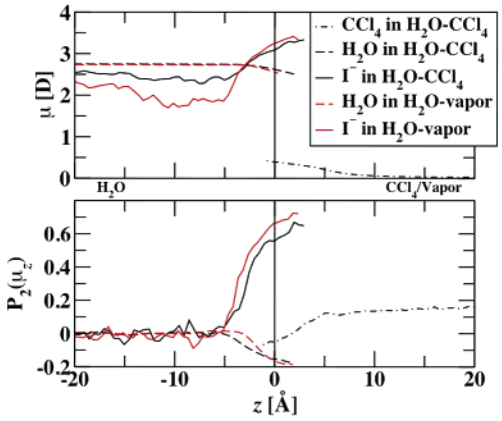

Figure 6. Magnitude of total dipole moment (top) and second moment of the orientational distribution for the total dipole moment with the *z*-axis (bottom) as a function of position for the 1 M CsI systems.

solvation shell), the oxygen−hydrogen distance was less than 2.4 Å, and the oxygen−hydrogen−oxygen angle was greater than 140°. For iodide−water hydrogen bonds, they were defined when the iodide−oxygen distance was less than 4.1 Å (defined as first solvation shell), the iodide−hydrogen distance less than 3.1 Å, and the oxygen−hydrogen−iodide angle was greater than 140°. The number of hydrogen bonds decreases at the interface for both water and iodide ions, but to a higher degree for water. In addition, the degree of hydrogen bonding decreases more for water in the H_2O−vapor system than in H_2O-CCl_4. A study by Benjamin argued that first shell ion solvation structure does not change as an ion approaches the interface from the bulk.[9] The current study suggests that for our system, the number of hydrogen bonds surrounding iodide decreases slightly as it approaches the interface. Another study by Dang and Chang calculated the hydration numbers of cesium and chloride as it approached the H_2O-CCl_4 interface,[25] and found a small decrease in hydration numbers as they approached the interface. The current study and the Dang and Chang study find little differences in solvation structure for ions as they approach the interface, unlike water, which has a significant difference in the number of hydrogen bonds at the interface compared to the bulk.

The ratio of hydrogen bonds increases for both water and iodide, but it is much higher for iodide. Also, in the region somewhat inside the interface, there is a significant drop in the ratio of hydrogen bonding for iodide in the H_2O−vapor system, which subsequently is in the region where cesium density is greater than iodide density.

C. Electrostatic and Orientational Properties. The magnitude of the overall molecular dipole for all species except cesium as a function of position for the 1 M CsI H_2O-CCl_4 and H_2O−vapor systems is given in Figure 6. In addition, Figure 6 gives the orientation of the dipole with respect to the *z*-axis as a function of distance, which was studied by determining the second moment of the orientational distribution function[26]

$$P_2 = \frac{1}{2}[3\cos\theta_z - 1] \qquad (2)$$

where θ_z represents the angle between the dipole of an individual molecule with the *z*-axis. The P_2 function will be zero for an unoriented system, one for a system fully oriented with the *z*-axis, and −0.5 for a system fully oriented perpendicular to the *z*-axis or parallel to the interface. The values for the pure and 3 M CsI H_2O-CCl_4 systems are not shown for clarity, and

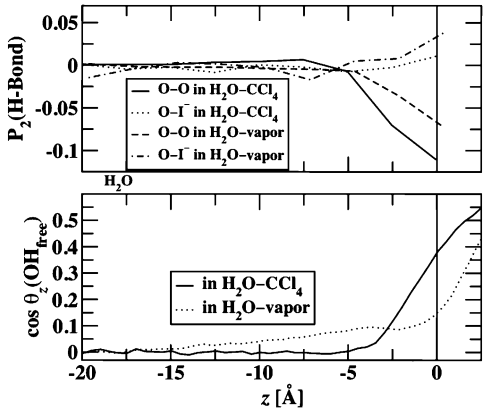

Figure 7. Second moment of the orientational distribution with the *z*-axis (top) of the vector formed from hydrogen bond donor hydrogens with oxygen and iodide, and the angle of free O−H bonds with the *z*-axis (bottom).

are nearly identical with the 1 M CsI H_2O-CCl_4 system for all species. Also, cesium (not shown for clarity) had a dipole of 0.28 D throughout the whole aqueous phase, and did not orient significantly in any region. For both systems, the water dipole decreases at the interface and orients parallel to the interface, which has been observed previously for aqueous ionic systems.[27] Iodide behaves differently, with its dipole increasing significantly at the interface, and orienting perpendicular to the interface, similar to what has been observed for chloride at the vapor−liquid interface.[27] Furthermore, the iodide dipole orients perpendicular to the interface more strongly in the H_2O−vapor system, and has a bigger difference between the bulk and interfacial dipole magnitudes. CCl_4 has an increased dipole in the interfacial region, which has been observed previously,[20] and its dipole is oriented slightly parallel to the interface in the interfacial region. Away from the interface, CCl_4 dipoles orient moderately along the *z*-axis, which is likely a system size effect present in the H_2O-CCl_4 system. The presence of the interface apparently creates a weak long-ranged ordering of dipoles along the *z*-axis that is not strong enough to significantly affect the dipole of water in the bulk, which is at least an order of magnitude greater than the CCl_4 dipole.

Figure 7 shows the second moment of the orientational distribution function for the hydrogen bonding angle with the *z*-axis for water and iodide in the 1 M CsI H_2O-CCl_4 and H_2O−vapor systems. The angle is determined from the vector from donor water hydrogens with another water oxygen or iodide ion. For instance, if the hydrogen−iodide vectors of all donating hydrogen bonding waters with iodide are perpendicular to the interface (aligned with the *z*-axis), the value of the function will be one. The definition for hydrogen bonds is the same as that given previously. Water−water hydrogen bonds are shown to orient somewhat parallel to the interface in the interfacial region, and more strongly in the H_2O-CCl_4 system. Hydrogen bonds with iodide orient slightly perpendicular to the interface near the Gibb's dividing surface. This is expected, since the dipole for iodide increases significantly at the interface, and orients strongly perpendicular to the interface. A previous study showed hydrogen bonds with chloride ions oriented much more strongly perpendicular to the interface,[27] in contrast to the results here. Iodide, though, is much larger than chloride, and accepts around four hydrogen bonds at the interface. If both iodide and chloride ions accept one very strong hydrogen bond aligned with its induced dipole, the larger size of iodide allows it to accept additional hydrogen bonds that are not aligned with its dipole than does chloride.

Figure 7 gives the angle of free O−H vectors with the vector pointing along the *z*-axis (perpendicular to the interface) away from the water center of mass. The higher the value, the more the free O−H vectors are oriented away from the bulk of the water phase. Free O−H's are defined from hydrogens that are not directly participating in hydrogen bonds (the other hydrogen may be), which are determined by using the previous hydrogen bonding definition for oxygen−oxygen and oxygen−hydrogen distances. The pure and 3 M H_2O-CCl_4 systems gave nearly identical results as the 1 M H_2O-CCl_4 system shown here, which is not shown for clarity. First of all, there is strong orientation of free O−H vectors away from the water bulk for all systems, in agreement with experimental observations for H_2O-CCl_4 and H_2O−vapor systems.[28] This effect is stronger for the H_2O-CCl_4 system than for H_2O−vapor, also in agreement with experimental observations.[28] This is likely the result of weak interactions of water hydrogens with CCl_4 chlorides, causing greater orientation of non-hydrogen bonding hydrogens toward the CCl_4 phase than otherwise would occur. In addition, the O−H vector orients toward the vapor phase even a moderate amount within the H_2O−vapor interface. The high anion density at the interface, coupled with increased cation density in the bulk region adjacent to the interface creates an electric field, in which water hydrogens orienting toward the interface would offset.

The electric field can be determined from a combination of the magnitude of the induced dipoles arising from the polarizabilties and the charge densities[29,30]

$$E(z) = \frac{1}{\epsilon_0}[-\langle\rho_\mu^{\mathrm{ind}}(z)\rangle + \int_B^{\mathrm{H_2O}} \langle\rho_q(z)\rangle\, dz] \qquad (3)$$

where $\rho_q(z)$ is the charge density, and $\rho_m^{\mathrm{ind}}(z)$ is the induced dipole density that is evaluated from the *z* component of the induced dipole pointing toward the water center of mass (i.e., a positive value represents dipoles pointing toward the water center of mass). The position of the induced dipole density is determined from the position of the point polarizability. For instance, water's point polarizability is on its *m* site, and for the ions, their point polarizabilities are located on their atomic position. The integral on the right-hand side of the equation is from either the center of mass of the CCl_4 phase or the vapor phase toward the water center of mass. The electric field is integrated along the *z*-axis toward the water center of mass to determine the potential drop

$$\Delta\Phi(z) = -\int_B^{\mathrm{H_2O}} E(z)\, dz \qquad (4)$$

The electric field as a function of position derived from both charge densities and induced dipoles for the 1 and 3 M CsI H_2O-CCl_4 systems and the 1 M H_2O−vapor system are given in Figure 8. The results for the pure H_2O-CCl_4 showed significantly less structure than the other systems and are not shown here for clarity. The electric field derived from charge density decreases with increasing ion concentration. This is expected from the specific density distributions, which show charge separation at the interface, with iodide being much more prevalent at the interface (which would cause a decrease in the electric field). Furthermore, the 1 M CsI H_2O−vapor system shows a decrease in its charge density derived electric field similar to that of the 3 M CsI H_2O-CCl_4 system, which is not unexpected because the iodide concentration at the interface is similar for the two systems. It can also be observed that the electric field is affected somewhat within the CCl_4 phase,

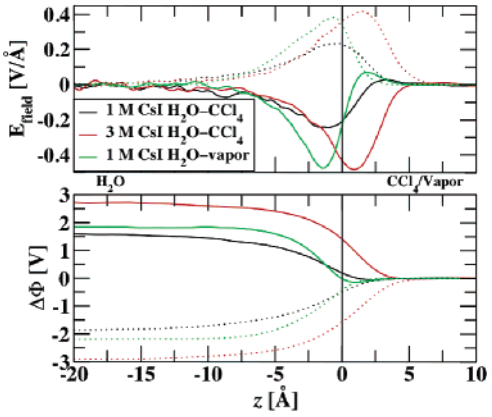

Figure 8. Electric field (top) and potential drop (bottom) as a function of position from charge distributions (solid lines) and induced dipoles (dotted lines).

resulting in the electric field profile being shifted to the right (or away from the H_2O center of mass) in the H_2O-CCl_4 systems compared to H_2O−vapor. The electric field from the induced dipoles is positive, being opposite of what is observed for the charge density electric field, and the induced dipole electric field increases with ion concentration. The increase in the electric field with increasing ion concentration is strongly influenced by iodide ions at the interface having their dipoles induced from hydrogen bonds from the waters located toward the bulk. This observation is consistent with Figure 6, which showed that at the interface for all systems, iodide has an induced dipole that is strongly oriented perpendicular to the interface.

The potential drop as a function of position from both charge distributions and induced dipoles is given in Figure 8. The total potential drop, including both charge and induced dipole contributions, at 20 Å from the Gibbs dividing surface in the aqueous phase for the pure, 1 M CsI, and 3 M CsI H_2O-CCl_4 systems, and the 1 M CsI H_2O−vapor system are −0.37, −0.28, −0.2, and −0.2 V, respectively. A potential drop for the pure H_2O−vapor system of −0.5 V was calculated in recent work with the Dang−Chang water model.[31] From these results, it is evident that increasing ion concentration results in an increase in the total potential drop for both H_2O-CCl_4 and H_2O−vapor systems. Previous experimental results found a small increase in potential drop for air−water interfaces with the addition of 1 M KI to pure water (around 0.07 V),[32] which is somewhat less than the calculated difference between the pure and 1 M CsI H_2O-CCl_4 systems (0.11 V) and the pure and 1 M CsI H_2O−vapor systems (0.15 V). However, the same trend is shown between simulation and experiment, and considering the differing systems, the agreement is quite good. It is interesting to note that the potential drops and electric fields change until around 10 Å from the Gibbs dividing surface in the aqueous phase. Also, the potential drop from induced dipoles is of very similar magnitude to the potential drop from static charges. Previous simulations showed very little change in the potential drop at a liquid−liquid interface with inclusion of ions with no polarization.[15] This result was expected because very little charge layering was present in the simulation. Although there is significant charge layering in the current study, the offsetting effect of the induced dipoles results in a relatively small change in the overall potential drop, which in a way disguises the significance of charge layering on the potential drop.

D. Hydrogen Bonding. Hydrogen bonding in the bulk and interfacial regions was studied by observing the distance and angular distributions between hydrogen bonded species. A

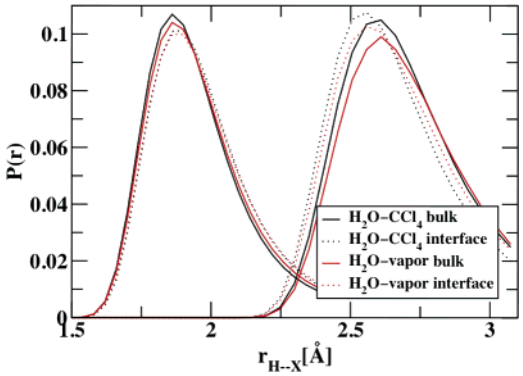

Figure 9. Oxygen−oxygen (left) and oxygen−iodide (right) distance distributions for hydrogen bonded species.

hydrogen bond between two waters in this case was defined if their oxygen−oxygen distance was less than 3.4 Å, their hydrogen−oxygen distance was less than 2.4 Å, and the angle formed from the bonded hydrogen−oxygen vector with the other water oxygen was greater than 140°. A hydrogen bond between a water and iodide was defined if their water−iodide distance was less than 4.1 Å, their hydrogen−iodide distance was less than 3.1 Å, and their oxygen−hydrogen−iodide angle was greater than 140°. A larger value of 155° for the minimum angle for a hydrogen bond was tested as well, and gave qualitatively similar results to those presented here. The distribution was determined by normalizing over all hydrogen bonded pairs meeting the stated criteria (giving a probability per pair).

Figure 9 presents the hydrogen−oxygen and hydrogen−iodide distance distributions for hydrogen bonded species for the bulk and interfacial regions for the 1 M CsI H_2O-CCl_4 and H_2O−vapor systems. The interfacial region was defined as between −5 (in the water phase) and 2.5 Å of the Gibb's dividing surface. The distributions show that for water−water hydrogen bonds, their intermolecular oxygen−hydrogen distance distribution peaks were somewhat lower and shifted to larger values at both the H_2O-CCl_4 and H_2O−vapor interfaces when compared with bulk. This suggests that hydrogen bonding is weaker at the interface for both systems, which has been observed experimentally for H_2O-CCl_4,[33] but not for H_2O−vapor, which was found to have stronger interfacial hydrogen bonds.[28] Moreover, while the oxygen−hydrogen distributions differ in the bulk region between the two systems, with H_2O-CCl_4 showing a narrower distribution, both systems behave very similar in the interfacial region. Oxygen−hydrogen distance distributions were also determined for the pure and 3 M CsI H_2O-CCl_4 systems, which gave distributions nearly identical with those shown for the 1 M CsI H_2O-CCl_4 system. The water−iodide distributions show a different story, in which their peaks become higher and shifte to shorter distances at both interfaces.

Table 1 presents the standard deviation of the angular distribution between a target water oxygen−hydrogen bond vector and a nonbonded oxygen or iodide atom that the target water is donating a hydrogen bond to. The criteria for a hydrogen bond are the same as those previously suggested, except with no angular constraints. Qualitatively, a larger standard deviation corresponds to a broader angular distribution. The water−water angular distributions have higher deviations at the interface than in the bulk for all systems studied. This is expected from the distance distribution results, since they showed lower peaks and longer distances at the interface compared with the bulk. Also, the water−iodide angular distributions have the opposite trend as water for the H_2O-

TABLE 1: Standard Deviation of the Distribution Formed from the Cosine of the Angle between Water Hydrogen−Oxygen Bond Vectors and Intermolecular Hydrogen Bonded Species (the mean for all cases is 180° or cos $q = -1$)

system	species	bulk	interface
pure H_2O-CCl_4	H_2O	0.0846	0.0870
1 M CsI H_2O-CCl_4	H_2O	0.0849	0.0870
	I^-	0.0744	0.0699
3 M CsI H_2O-CCl_4	H_2O	0.0858	0.0876
	I^-	0.0747	0.0684
1 M CsI H_2O−vapor	H_2O	0.0864	0.0881
	I^-	0.0863	0.0865

TABLE 2: Diffusion Parallel (*xy*) and Perpendicular (*z*) to the Interface in the Bulk and Interfacial Regions[a,b]

		bulk		interface	
system	species	D_{xy}	D_z	D_{xy}	D_z
pure H_2O-CCl_4	CCl_4	0.198_5	0.215_{14}	0.192_7	0.153_{13}
	H_2O	0.150_3	0.156_4	0.186_{10}	0.180_{16}
1 M CsI H_2O-CCl_4	CCl_4	0.198_2	0.209_{16}	0.197_4	0.166_{22}
	H_2O	0.151_3	0.157_4	0.174_3	0.212_8
	Cs^+	0.139_6	0.144_3	0.128_2	0.116_{17}
	I^-	0.111_3	0.119_9	0.129_5	0.134_{12}
3 M CsI H_2O-CCl_4	CCl_4	0.196_4	0.226_{13}	0.209_7	0.180_2
	H_2O	0.148_2	0.159_4	0.147_2	0.166_{12}
	Cs^+	0.131_4	0.159_8	0.121_8	0.158_{20}
	I^-	0.102_4	0.114_7	0.115_7	0.131_{12}
1 M CsI H_2O−vapor	H_2O	0.180_{11}	0.194_5	0.29_3	0.36_5
	Cs^+	0.194_{10}	0.156_{24}	0.24_3	0.31_9
	I^-	0.194_7	0.154_{26}	0.25_3	0.15_4

[a] Subscripts represent uncertainty in the last digit(s). [b] Units: $Å^2\ ps^{-1}$.

CCl_4 system, with higher deviations in the bulk compared with the interface, similar to the observations made in the distance distributions. In the H_2O−vapor system, though, the angular deviations are almost identical in the interface and bulk.

The origin for the general discrepancies of hydrogen bonding between the interface and bulk can be traced to the fact that water dipoles decrease at the interface, and iodide dipoles increase at the interface. A stronger induced dipole on a heavy atom would most likely increase the strength of accepted hydrogen bonds, provided that the hydrogen bond is properly aligned with the dipole.

E. Dynamics. The translational diffusion was determined in regions distributed in 2.5 Å slabs along the *z*-axis for movement parallel and perpendicular to the interface. The technique used to calculate diffusion parallel and perpendicular to the interface has been detailed previously.[27,34] The diffusion coefficients parallel to the interface are calculated with use of the Einstein relation, and the coefficients perpendicular to the interface are calculated by using a dual simulation technique, using a combination of molecular dynamics and Langevin dynamics. For further details see ref 24. Diffusion coefficients were determined in 6 ps time intervals, after 3 ps of time had expired for the specific interval.

Table 2 gives the diffusion coefficients for all molecular species in all systems in the interfacial and bulk regions. For translational dynamics, the interfacial region was defined between −5 and 0 Å from the Gibb's dividing surface for water, cesium, and iodide, and between 0 and 5 Å for CCl_4, where negative values correspond with the water phase. The results show that water is fairly isotropic in the bulk region, but has higher diffusion rates perpendicular to the interface (along the *z*-axis) for the 3 M CsI H_2O-CCl_4 system and the 1 M H_2O−vapor system. Figure 8 showed that the electric field from induced dipoles is positive well into the bulk primarily for these two systems, which should increase the intermolecular interactions along the *z*-axis. With this increase in interaction, it should result in the liquid being "stiffer" in the *z* direction compared to the *xy* direction. With use of a vacancy model for diffusion, it would be more difficult to find a vacancy in directions with greater stiffness, slowing diffusion in the directions with greater stiffness. Water has slightly faster diffusion in the interfacial region than in the bulk for the H_2O-CCl_4 systems. This is likely due to the fact that diffusion is faster in the CCl_4 phase, and water molecules in the interface are in contact with both water and CCl_4, resulting in slightly faster overall diffusion than in bulk water.

The CCl_4 bulk shows a discrepancy between diffusion perpendicular and parallel to the interface as well, with perpendicular diffusion being faster than parallel diffusion. Figure 6 showed that the CCl_4 dipole was moderately oriented perpendicular to the interface throughout the bulk CCl_4 region, which again should cause increased stiffness along the *z* direction. By using the same arguments as for water, this should result in faster diffusion along the *z* direction than the *xy* direction. At the interface, CCl_4 diffusion is faster parallel to the interface than perpendicular to the interface. A single CCl_4 at the interface would most likely be in contact with other CCl_4's in three directions, and with water in one direction. The hydrogen bonding water phase is stiffer than the CCl_4 phase, and would likely impede the movement of CCl_4, somewhat reducing the perpendicular diffusion of CCl_4.

Cesium and iodide diffusion is fairly isotropic in the water bulk for the H_2O-CCl_4 systems. The parallel diffusion is faster than the perpendicular diffusion in the bulk of the H_2O−vapor system, but the low concentration of the species in the bulk and high uncertainties do not allow this result to be conclusive. At the interface, cesium is isotropic, but iodide has faster diffusion parallel to the interface than perpendicular. Iodide has strong induced dipoles oriented perpendicular to the interface, which should promote extra strong hydrogen bonds with waters primarily in this direction. Figure 7 showed a small increase in the probability for a hydrogen bonding water to be located in the region perpendicular to the interface. With use of a vacancy model for diffusion, the presence of a water in this region will impede iodide diffusion perpendicular to the interface, but also impede the diffusion of other species parallel to the interface, since these stronger hydrogen bonds should increase the stiffness of the liquid perpendicular to the interface. This compensation of effects clearly works to decrease iodide perpendicular diffusion with respect to parallel diffusion, in which nearly all iodide molecules are likely to experience these strong and perpendicularly oriented hydrogen bonds. This is similar to what has been observed for the diffusion of chloride at the H_2O−vapor interface.[27] For interfacial waters, though, many will not be directly contributing to the strong hydrogen bonding with iodide, since many will be located close to the same *z* coordinate as iodide (which by definition are not forming hydrogen bonds perpendicular to the interface with the iodide). Because of this, interfacial water diffusion will be slowed parallel to the interface with respect to perpendicular diffusion due to the increased stiffness along the *z* direction caused by the extra strong water−iodide hydrogen bonds. Water's anisotropic diffusion is observed at the interface for all systems with ions, but not for the pure H_2O-CCl_4 system or with previous studies of pure water and argon vapor−liquid interfaces,[34] showing consistency with the argument.

Rotational autocorrelation functions for the 1 M CsI H_2O-CCl_4 and H_2O−vapor systems were calculated in 2.5 Å slabs

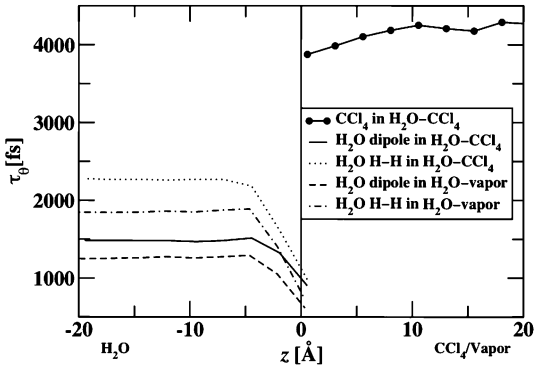

Figure 10. Rotational decorrelation times as a function of position for CCl_4, the water dipole vector, and the water hydrogen−hydrogen vector.

spaced along the *z*-axis for the CCl_4 C−Cl bond vector, water dipole vector, and water H−H vector. The time it takes for the autocorrelation functions to reach exp(−1) is plotted as a function of position in Figure 10. A molecule is considered to be in a certain region if it spends a majority of its time in that region. If a molecule leaves a region before its autocorrelation function reaches exp(−1), it is still counted, otherwise the results would be biased toward smaller numbers (there would be a lower probability to include molecules with faster diffusion). Because of this, the value shown for a specified region will be somewhat influenced by adjacent regions, but qualitative trends can be extracted from the results.

The CCl_4 decorrelation times decreased slightly toward the interface, showing faster rotational diffusion at the interface, in contrast with what was observed for translational diffusion. The water dipole and H−H vectors decorrelate significantly faster at the interface for both the H_2O-CCl_4 and H_2O−vapor systems. This is consistent with the translational diffusion results, which showed faster diffusion at the interface. The water rotational decorrelation time is faster for the bulk of the H_2O−vapor system than for the H_2O-CCl_4 system, again consistent with the translational diffusion results.

IV. Conclusions

Molecular dynamics simulations were carried out to understand ion distributions, structural properties, and dynamics at different CsI concentrations in H_2O−vapor and H_2O-CCl_4 interfacial systems. Iodide was very surface active at the H_2O−vapor interface, and moderately surface active at the H_2O-CCl_4 interface, which was found to be the result of an increase in the induced dipole of iodide, leading to stronger hydrogen bonds at the interface. Iodide was also found to have short to moderate ranged repulsion with CCl_4, causing a decrease in iodide H_2O-CCl_4 interface activity when compared with the H_2O−vapor interface. Water−water hydrogen bonding was found to be weaker at both interfaces, which agrees with experiment for H_2O-CCl_4, but not for H_2O−vapor.[28] It should be noted that one recent vibrational sum-frequency spectroscopy measurement found no evidence of anion enhancement at the H_2O−vapor interface,[12] but another study did find evidence of higher concentrations of bromide and iodide ions at the interface compared to the bulk.[14] Recent techniques calculating sum-frequency spectroscopy directly from molecular dynamics simulations would be useful in resolving these disagreements.[10,35,36] Translational and rotational diffusion was faster at both interfaces for water, but CCl_4 diffusion had faster rotational diffusion but slower translational diffusion at the interface. For many species and systems, translational diffusion was anisotropic at both the interface and bulk.

Acknowledgment. This work was performed at Pacific Northwest National Laboratory (PNNL) under the auspices of the Division of Chemical Sciences, Office of Basic Energy Sciences, U.S. Department of Energy. Battelle operates PNNL for the Department of Energy.

References and Notes

(1) McLaughlin, S. *Annu. Rev. Biophys. Biophys. Chem.* **1989**, *18*, 113.
(2) Honig, B. H.; Hubbell, W. L.; Flewelling, R. F. *Annl. Rev. Biophys. Biophys. Chem.* **1986**, *15*, 163.
(3) *Biophysics of Water*; Franks, Mathias, S., Ed.; Wiley-Interscience: New York, 1982.
(4) Knipping, E. M.; Lakin, M. J.; Foster, K. L.; Jungwirth, P.; Tobias, D. J.; Gerber, R. B.; Dabdub, D.; Finlayson-Pitts, B. J. *Science* **2000**, *288*, 301.
(5) Haag, W. R.; Yao, C. C. D. *Environ. Sci. Technol.* **1992**, *26*, 1005.
(6) Jungwirth, P.; Tobias, D. J. *J. Phys. Chem. B* **2002**, *106*, 6361.
(7) Mucha, M.; Frigato, T.; Levering, L. M.; Allen, H. C.; Tobias, D. J.; Dang, L. X.; Jungwirth, P. *J. Phys. Chem. B* **2005**, *109*, 7617.
(8) Dang, L. X. *J. Phys. Chem. B* **2002**, *106*, 10388.
(9) Benjamin, I. *J. Chem. Phys.* **1991**, *95*, 3698.
(10) Brown, E. C.; Mucha, M.; Jungwirth, P.; Tobias, D. J. *J. Phys. Chem. B* **2005**, *109*, 7934.
(11) Ghosal, S.; Hemminger, J. C.; Bluhm, H.; Mun, B. S.; Hebenstreit, E. L. D.; Ketteler, G.; Ogletree, D. F.; Requejo, F. G.; Salmeron, M. *Science* **2005**, *307*, 563.
(12) Raymond, E. A.; Richmond, G. L. *J. Phys. Chem. B* **2004**, *108*, 5051.
(13) Petersen, P. B.; Saykally, R. J. *Chem. Phys. Lett.* **2004**, *397*, 51.
(14) Liu, D. F.; Ma, G.; Levering, L. M.; Allen, H. C. *J. Phys. Chem. B* **2004**, *108*, 2252.
(15) Fernandes, P. A.; Cordeiro, M.; Gomes, J. *J. Phys. Chem. B* **2001**, *105*, 981.
(16) Schnell, B.; Schurhammer, R.; Wipff, G. *J. Phys. Chem. B* **2004**, *108*, 2285.
(17) U.S. Department of Energy, Office of Environmental Management, FY 1995 Technology Development Needs Summary, 1994.
(18) Dang, L. X.; Chang, T. M. *J. Chem. Phys.* **1997**, *106*, 8149.
(19) Dang, L. X.; Chang, T. M.; Panagiotopoulos, A. Z. *J. Chem. Phys.* **2002**, *117*, 3522.
(20) Chang, T. M.; Dang, L. X. *J. Chem. Phys.* **1996**, *104*, 6772.
(21) Ryckaert, J. P.; Ciccotti, G.; Berendsen, H. J. C. *J. Comput. Phys.* **1977**, *23*, 327.
(22) Smith, D. E.; Dang, L. X. *J. Chem. Phys.* **1994**, *101*, 7873.
(23) Berendsen, H. J. C.; Postma, J. P. M.; Vangunsteren, W. F.; Dinola, A.; Haak, J. R. *J. Chem. Phys.* **1984**, *81*, 3684.
(24) Matsumoto, M.; Kataoka, Y. *J. Chem. Phys.* **1988**, *88*, 3233.
(25) Dang, L. X.; Chang, T. M. Mass transport across liquid/liquid interfaces. In *Water in Confining Geometries*; Buch, V., Devlin, J. P., Eds.; Springer: Berlin, Germany, 2003; p 243.
(26) de Gennes, P. G.; Prost, J. *The Physics of Liquid Crystals*, 2nd ed.; Clarendon Press: Oxford, UK, 1993.
(27) Wick, C. D.; Dang, L. X. *J. Phys. Chem. B* **2005**, *109*, 15574.
(28) Scatena, L. F.; Richmond, G. L. *J. Phys. Chem. B* **2001**, *105*, 11240.
(29) Schweighofer, K. J.; Benjamin, I. *Chem. Phys. Lett.* **1993**, *202*, 379.
(30) Wilson, M. A.; Pohorille, A.; Pratt, L. R. *J. Chem. Phys.* **1988**, *88*, 3281.
(31) Randles, J. E. B. *Phys. Chem. Liq.* **1977**, *7*, 107.
(32) Dang, L. X.; Chang, T. M. *J. Phys. Chem. B* **2002**, *106*, 235.
(33) Scatena, L. F.; Brown, M. G.; Richmond, G. L. *Science* **2001**, *292*, 908.
(34) Liu, P.; Harder, E.; Berne, B. J. *J. Phys. Chem. B* **2004**, *108*, 6595.
(35) Morita, A.; Hynes, J. T. *J. Phys. Chem. B* **2002**, *106*, 673.
(36) Perry, A.; Ahlborn, H.; Space, B.; Moore, P. B. *J. Chem. Phys.* **2003**, *118*, 8411.